AD-A096 355 OHIO STATE UNIV RESEARCH FOUNDATION COLUMBUS F/G 20/4
SPECTRAL COMPUTATION OF TRIPLE-DECK FLOWS.(U)
JAN 81 O R BURGGRAF N00014-76-C-0333
UNCLASSIFIED TR-3 NL

END
DATE FILMED
4-81
DTIC

RF Project 760325/712792
Technical Report 3

the ohio state university
research foundation
1314 kinnear road
columbus, ohio
43212

SPECTRAL COMPUTATION OF TRIPLE-DECK FLOWS

Odus R. Burggraf
Department of
Aeronautical and Astronautical Engineering

Department of the Navy
Office of Naval Research
Arlington, Virginia 22217

Contract N00014-76-C-0333

January, 1981

Unclassified

SECURITY CLASSIFICATION OF THIS PAGE (When Data Entered)

REPORT DOCUMENTATION PAGE	READ INSTRUCTIONS BEFORE COMPLETING FORM
1. REPORT NUMBER	2. GOVT ACCESSION NO. AD-A096 355 / 3. RECIPIENT'S CATALOG NUMBER
4. TITLE (and Subtitle) SPECTRAL COMPUTATION OF TRIPLE-DECK FLOWS	5. TYPE OF REPORT & PERIOD COVERED Technical #3 12/1/78-12/31/80
	6. PERFORMING ORG. REPORT NUMBER 760325/712792
7. AUTHOR(s) Odus R. Burggraf	8. CONTRACT OR GRANT NUMBER(s) N00014-76-C-0333
9. PERFORMING ORGANIZATION NAME AND ADDRESS The Ohio State University Research Foundation, 1314 Kinnear Road Columbus, Ohio 43212	10. PROGRAM ELEMENT, PROJECT, TASK AREA & WORK UNIT NUMBERS
11. CONTROLLING OFFICE NAME AND ADDRESS	12. REPORT DATE Jan[redacted]81
	13. NUMBER OF PAGES 10
14. MONITORING AGENCY NAME & ADDRESS (if different from Controlling Office)	15. SECURITY CLASS. (of this report) Unclassified
	15a. DECLASSIFICATION DOWNGRADING SCHEDULE

16. DISTRIBUTION STATEMENT (of this Report)

Approved for public release; distribution unlimited

17. DISTRIBUTION STATEMENT (of the abstract entered in Block 20, if different from Report)

18. SUPPLEMENTARY NOTES

19. KEY WORDS (Continue on reverse side if necessary and identify by block number)

computational fluid dynamics, viscous interaction, boundary layer, spectral method, triple-deck flows

20. ABSTRACT (Continue on reverse side if necessary and identify by block number)

The Fourier transform method is applied to the problem of computing viscous flows involving boundary-layer separation, based on the triple-deck model of viscous-inviscid flow interaction. As used here, the method is pseudo-spectral in that the non-linear inertia terms are evaluated in physical variables, although the main computations are made in spectral variables. The Fast-Fourier-Transform algorithm is used to expedite the interated transformations. The method is much faster than conventional finite-difference

(continued)

DD FORM 1 JAN 73 1473

Unclassified

SECURITY CLASSIFICATION OF THIS PAGE (When Data Entered)

26736-0

Block 20 (Abstract) - Continued

methods; typically only ten or twenty interations suffice for convergence to four or five digits of accuracy. Furthermore, no artificial stabilization schemes are necessary to treat the reversed flows occurring in separated regions. Results are presented for both incompressible and supersonic flows, and are shown to compare well with previous finite-difference results.

ACKNOWLEDGEMENT

This paper was prepared for the Symposium on Physical and Numerical Aspects of Aerodynamic Flows held at California State University at Long Beach, January 20-22, 1981.

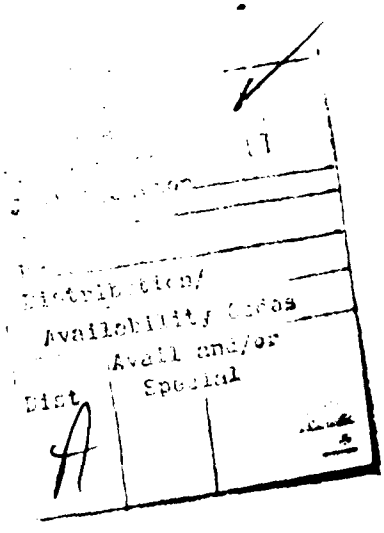

SPECTRAL COMPUTATION OF TRIPLE-DECK FLOWS

Odus R. Burggraf
The Ohio State University, Columbus, Ohio

and

P. W. Duck*
University of Manchester, England

Abstract

The Fourier transform method is applied to the problem of computing viscous flows involving boundary-layer separation, based on the triple-deck model of viscous-inviscid flow interaction. As used here, the method is pseudo-spectral in that the nonlinear inertia terms are evaluated in physical variables, although the main computations are made in spectral variables. The Fast-Fourier-Transform algorithm is used to expedite the iterated transformations. The method is much faster than conventional finite-difference methods; typically only ten or twenty iterations suffice for convergence to four or five digits of accuracy. Furthermore, no artificial stabilization schemes are necessary to treat the reversed flows occurring in separated regions. Results are presented for both incompressible and supersonic flows, and are shown to compare well with previous finite-difference results.

I. Introduction

In recent times the most common means of solving (numerically) Prandtl's boundary-layer equations has been finite-difference marching methods. Despite the nonlinearity of these equations, these techniques (incorporating Newton iteration) can provide rapid accurate solutions on modern computers. The marching method was applied successfully, for example, by Jobe and Burggraf[1] in their solution of the triple-deck problem of interaction between boundary layer and free stream near a trailing edge. Nevertheless, there are several types of flow for which these marching techniques either fail or become difficult to implement. Of these difficult types, perhaps separated flow is the most obvious. The physical cause of the difficulty is the region of reversed flow, in which the fluid travels in the direction opposite to that of the main body of fluid. As a result there is a change of character of the governing boundary-layer equations. Usually these are of parabolic type for which marching techniques are valid; however, the flow reversal due to separation changes the nature of the boundary-layer equations to quasi-elliptic type, with information being propagated both upstream and downstream. Any attempt to obtain an accurate solution by marching through such reversed-flow regions must fail due to the improper direction of information flow. In finite-difference procedures, the failure is usually exhibited either by lack of convergence of the iterative procedure or by severe oscillations in the "solution".

Reyhner and Flügge-Lötz[2] have demonstrated a simple, though approximate, remedy to this problem of treating reversed flows. Their approximation was to neglect the product of the streamwise velocity component u and its streamwise derivative u_x in the governing equations wherever u became negative. This technique has been used by a number of authors[3,4] with good results for the computed pressure distribution. However, much of the success of this technique owes to the fact that the reversed flow is very

*Formerly, Research Associate, The Ohio State University. This work was sponsored by Office of Naval Research under Contract N00014-76-C-0333.

slow in many situations, and so the exclusion of this component of the inertia terms is of little consequence in those cases.

Williams[5] has suggested a more rational (and more complicated) procedure for treating reversed flows based on bidirectional marching techniques. The Reynner and Flügge-Lötz (FLARE) procedure is used as a first approximation, followed by a backwards sweep in the reversed-flow region only. The previously neglected uu_x term in the reversed-flow region is now accounted for in the next forward sweep by treating it as a known quantity evaluated from the preceding backwards sweep. This downstream-upstream iteration (DUIT) is then continued until convergence is achieved. Williams usually finds only five to ten of these sweeps to be necessary. Obviously this method is considerably less straightforward to program than simple marching procedures, and also takes rather longer to compute.

Another class of problems for which the standard marching techniques require iterative application is that to free-interaction flows. Originally postulated by Lighthill[6], these flows are essentially eigensolutions of the boundary-layer equations that provide the means of upstream influence in the flow, despite the parabolic nature of the governing equations. Stewartson and Williams[7] and later Smith and Stewartson[8] used a shooting approach to generate their free-interaction solutions. Here the pressure is perturbed by a small jump and the resulting solution is obtained by marching downstream; the correct amount of perturbation is determined such that the free-interaction solution is suppressed far downstream. As usual with shooting methods, this approach proves more and more difficult as the range of integration is extended downstream, owing to the ultimate exponential growth of the free-interaction solutions.

The above methods all solve the steady-flow equations by marching in the flow direction. An alternative is time-marching, with which the unsteady equations are integrated forward in time until a steady-state solution is obtained. This approach permits retention of all the inertia terms in the equations of motion, even in reversed-flow regions. Jenson, et al[9], and later Rizzetta, et al[10], applied the time-marching procedure to the triple-deck formulation for supersonic separated flows over ramp configurations. Their method was based on shear stress as the primary dependent variable. Upstream influence was then accounted for through an interaction condition applied as a wall boundary condition on the stress: namely, the boundary-layer compatibility condition with the pressure gradient evaluated from the displacement function. This condition is an exact requirement of the interacting flow, and permits downstream conditions to influence the upstream flow at each time step of the computation. The method works well but flows with extensive separation are rather expensive to compute due to their slow development in time. An interacting boundary-layer program based on similar ideas has been presented by Werle and Vatsa[11] and has been shown to give results that asymptote the triple-deck results for very large Reynolds number[12].

Various alternatives to these finite-difference approaches have been proposed. The spectral method seemed to us to have characteristics advantageous for computing separated flows, and we have applied it to the triple-deck problem in this study. The (nonlinear) governing equations are transformed from physical to spectral variables using the Fourier integral transform in the main-flow direction, together with finite-differences in the transverse direction. The solution is computed (iteratively) in spectral space and then the inverse transform applied to obtain the solution in physical variables. A major advantage of the method is that reversed flows present no difficulty; each point in spectral space relates to all points on the path of integration in

physical space. Thus the reversed and forward-flow information is diffused together in transform variables. This interconnection between the physical grid points via each spectral grid point endows the spectral method with a physically implicit nature, suggesting an accelerated convergence of the iterations. As will be seen, the spectral computations exhibit rapid convergence, even for flows exhibiting separated regions large enough that other (finite-difference) schemes fail.

Details of the method as well as results of computations for both incompressible and supersonic flows are given below. In both cases, the spectral results are shown to compare well with those of finite-difference computations.

II. The Mathematical Problem

The problem considered is the flow disturbance produced by a shallow perturbation of the surface height at a distance L from the leading edge of an otherwise plane wall. Let u_∞ be the flow speed and ν_∞ the kinematic viscosity of the fluid, the subscript (∞) referring to conditions in the undisturbed freestream. The Reynolds number $R = u_\infty L/\nu_\infty$ is regarded as large. As is common in triple-deck analyses, it is convenient to define the small parameter ϵ as $R^{-1/8}$. Then if the surface height perturbation is of order $\epsilon^5 L$ and extends over a length of order $\epsilon^3 L$, the flow disturbance is contained in the triple-deck structure originally deduced by Messiter[13], Neiland[14] and Stewartson[7]. Since this asymptotic flow structure has been described by many authors, we merely state here that the problem reduces to solving the conventional incompressible boundary-layer equations (governing the lower-deck flow) subject to an unconventional outer boundary condition whose form depends on whether the outer flow is incompressible or supersonic. (A hypersonic version exists as well, but is not considered in this work; See Ref. 15).

It is convenient to describe the triple-deck disturbance using variables with magnitude of order one. These are denoted by upper case letters while lower case letters designate the corresponding physical variable. Thus, the coordinate representing distance parallel to the surface is $x = \epsilon^3 aLX$ while the normal coordinate is $y = \epsilon^5 bLY$. The origin is taken at a convenient point on the disturbed surface. The corresponding velocity components are $u = \epsilon(d/b)u_\infty U$ and $v = \epsilon^3(d/a)u_\infty V$, while the pressure $p = p_\infty(1 + \epsilon^2 cP)$. Here a, b, c and d are constant scale factors depending on Mach number, wall-temperature ratio, and the surface stress of the undisturbed flow. Their values are given, for example, in Refs. 7 and 10 for supersonic flow, and in Refs. 1 and 16 for incompressible flow. Following Jenson, et al[9,10], we introduce the shear $\tau = U_Y$ as basic dependent variable, where subscripts denote partial derivatives. Then the equation to be solved in the lower deck is the shear transport equation,

$$U\tau_X + V\tau_Y = \tau_{YY} \qquad (1)$$

together with the continuity equation

$$U_X + V_Y = 0 \qquad (2)$$

The conventional no-slip conditions apply:

$$U = V = 0 \quad \text{on} \quad Y = 0 \qquad (3)$$

The remaining boundary conditions take a form governed by the triple-deck structure. Upstream the shear must match to that of the undisturbed flow near the wall; thus,

$$\tau \to 1 \quad \text{for} \quad X \to -\infty \qquad (4)$$

Moreover, the triple-deck structure requires that the main-deck solution correspond to a simple vertical displacement of the original undisturbed boundary layer by the lower deck. Consequently, matching of main and lower deck solutions requires

$$\tau \to 1 \quad \text{as} \quad Y \to \infty \qquad (5)$$

The corresponding condition for U is

$$U \sim Y + A(X) \quad \text{as} \quad Y \to \infty$$

where A(X) is the (negative) displacement of the main deck. For supersonic flow, the pressure is given by linearized potential theory as

$$P = H'(X) - A'(X)$$

where H(X) is the height of the surface perturbation in lower-deck scaling. The boundary-layer compatibility condition states that the pressure gradient balances the normal gradient of the shear at the wall. Expressing A in the form

$$A(X) = \lim_{Y\to\infty} (U - Y) = \int_0^\infty (\tau - 1)dY,$$

the compatibility condition for supersonic flow can then be expressed as

$$\tau_Y\Big|_{Y=0} = H''(X) - \int_0^\infty \tau_{XX}\, dY \qquad (6)$$

On the other hand, the elliptic nature of incompressible flow gives rise to a Hilbert integral for the pressure:

$$P(X) = \frac{1}{\pi} \int_{-\infty}^{\infty} \frac{H'(S) - A'(S)}{S - X} \qquad (7)$$

Thus, an interaction condition very similar to Eq. (6) can be given for incompressible flow. This will be postponed, however, as the similarity is much more remarkable in spectral variables.

The Fourier transform is now applied to the governing equations. Using an overbar to denote transformed variables, the transform $\bar{\phi}(\omega)$ of any real function $\phi(X)$ is given as

$$\bar{\phi}(\omega) \equiv F(\phi(X)) \equiv \int_{-\infty}^{\infty} \phi(X) e^{-i\omega X}\, dX$$

Actually to permit convergence of the integrals, the transformation is performed on the perturbation flow quantities. Define

$$\tilde{\tau} = \tau - 1$$

$$\tilde{U} = U - Y$$

$$\bar{\tilde{\tau}}(\omega, Y) = F\{\tilde{\tau}(X, Y)\}$$

$$\bar{\tilde{U}}(\omega, Y) = F\{\tilde{U}(X, Y)\}$$

$$\bar{V}(\omega, Y) = F\{V(X, Y)\}$$

In terms of these perturbation variables, the shear transport equation (1) becomes

$$Y\tau_X - \tau_{YY} = -(\tilde{U}\tau_X + V\tau_Y) \equiv R \qquad (8)$$

where the second-order perturbation terms have been placed on the right side of the equation. The spectral form of this equation is

$$i\omega Y\bar{\tilde{\tau}} - \bar{\tilde{\tau}}_{YY} = \bar{R} \equiv \overline{-(\tilde{U}\tau_X + V\tau_Y)} \qquad (9)$$

The right-side function $\bar{R}$ has the form of a complicated convolution integral. However, it need not be given here, since the term will be evaluated by another method (pseudo-spectrally). The continuity equation (2) is expressed spectrally as

$$\bar{V}_Y = -i\omega\bar{U} = -i\omega \int_0^Y \bar{\tau} dY \qquad (10)$$

The boundary conditions (3)-(6) also must be expressed in spectral variables. Thus,

$$\bar{U} = 0 \qquad \text{on} \quad Y = 0 \qquad (11)$$

$$\bar{V} = 0 \qquad \text{on} \quad Y = 0 \qquad (12)$$

$$\bar{\tau} \to 0 \qquad \text{as} \quad Y \to \infty \qquad (13)$$

and the interaction condition (6) for supersonic flow becomes

$$\bar{\tau}_Y\Big|_{Y=0} = -\omega^2(\bar{H}(\omega) - \int_0^\infty \bar{\tau}(\omega, Y)dY) \qquad (14)$$

For incompressible flow, the pressure is given by Eq. (7), so that the compatibility condition becomes

$$\bar{\tau}_Y\Big|_{Y=0} = i\omega\bar{P}$$

Applying the Fourier transform to the Hilbert integral in Eq. (7) thus yields the incompressible interaction condition

$$\bar{\tau}_Y\Big|_{Y=0} = -i\omega|\omega|(\bar{H}(\omega) - \int_0^\infty \bar{\tau}(\omega, Y)dY) \qquad (15)$$

which is very similar in form to the supersonic interaction condition. In fact, this slight difference between Eqs. (14) and (15) is the only difference in the triple-deck theories for supersonic and incompressible flow. Yet as will be demonstrated, large apparent differences in the physical flow properties result. The significance with regard to computer programming is that the change of a single FORTRAN statement permits computing either supersonic or incompressible flows with the same computer code.

III. The Solution Procedure

The spectral shear-transport equation (9) has been written in the form of a linear ordinary differential operator on the left side, with the non-linear inertia terms collected together into the right-side function $\bar{R}$. The solution is obtained by iteration, solving first with $\bar{R}$ set identically zero; then in later iterations $\bar{R}$ is evaluated from the subsequent solution, as

$$i\omega\bar{\tau}^{(n)} - \bar{\tau}_{YY}^{(n)} = \bar{R}^{(n-1)} = -(\bar{U}^{(n-1)}\tau_X^{(n-1)} + V^{(n-1)}\tau_Y^{(n-1)}) \qquad (16)$$

Central differences in Y are applied to Eq. (16), as well as to the interaction condition, either (14) or (15). The result of the first iteration is the linearized theory of Stewartson[17], which provides a reasonably accurate prediction for small disturbances. For disturbances large enough to produce flow separation, further iteration is necessary to bring in the effects of the non-linear inertia terms.

The right-side function $\bar{R}$ in Eq. (16) can be expressed as a convolution of the velocity referred to two different points in spectral space. However, evaluating this convolution integral is a very inefficient way of determining $\bar{R}$, requiring of order $N_Y N_\omega^2$ multiplications, for each complete iteration, where N_Y and N_ω are the number of grid points in the Y and ω (spectral) directions, respectively.

A much more efficient method is to use the so-called Fast Fourier Transform (FFT) algorithm of Cooley and Tukey[18]. The procedure used here is to invert the transforms $\bar{\tau}$ and $i\omega\bar{\tau}$ to obtain the physical variables τ and τ_X. From these $\bar{U}$, U_X, and V are determined, permitting the inertia function R of Eq. (8) to be evaluated. Applying the direct transform to R then results in the desired inertia transform term $\bar{R}$. Eq. (16) is then solved for the next approximation, and the above procedure is iterated until the solution repeats to the desired number of decimal places. The advantage of this method arises from the efficiency of the FFT algorithm; the scheme outlined here requires only of the order of $N_Y N_\omega \log_2 N_\omega$ multiplications for each complete iteration, compared with $N_Y N_\omega^2$ for the direct method based on the convolution integral. An order of magnitude reduction in computing time is achieved for quite reasonable grid resolution. It may be noted that the method used here is the reverse of the pseudo-spectral method described by Orszag[19] and Roache[20], who solve the equations of motion in the physical plane and use the Fourier transform to evaluate derivatives.

The discretization of the Fourier transforms was carried out as follows. Define the discrete physical and spectral variables X_j and ω_k as

$$X_j = (j-1-M)\Delta X \text{ for } j = 1,2,\ldots,N; \qquad (17a)$$

$$\omega_k = (k-1-M)\Delta\omega \text{ for } k = 1,2,\ldots,N; \qquad (17b)$$

where for convenience we take $N = 2M$. Denote any physical function $\phi(X_j)$ by ϕ_j, and the corresponding spectral function $\bar{\phi}(\omega_k)$ by $\bar{\phi}_k$. Choose the range of variables such that $\phi(X)$ is negligable for $X < X_1$, $X > X_{N+1}$, and $\bar{\phi}(\omega)$ is negligable for $\omega < \omega_1$, $\omega > \omega_{N+1}$. Then the Fourier

integral transform $\bar{\phi}(\omega)$, defined in the last section, can be approximated by the finite sum

$$\bar{\phi}_k = \Delta X \sum_{j=1}^{N} \phi_j \, e^{-i\omega_k X_j} \qquad (18)$$

The range of integration is slightly uncentered, from $X = -(M + 1/2)\Delta X$ to $X = (M - 1/2)\Delta X$. Since $\phi(X)$ is real, it follows from the form of the transform that $\bar{\phi}(-\omega) = \bar{\phi}^*(\omega)$, where the asterisk denotes the complex conjugate. Because of this property the transform variables need not be stored for, say, positive values of ω_k. The midrange parameter M in Eqs. (17) is now required to be an even integer and the grid spacings ΔX and $\Delta\omega$ satisfy the relation

$$\Delta X \Delta\omega = 2\pi/N \qquad (19)$$

Then, Eq. (18) can be reduced to the finite Fourier transform

$$\bar{\phi}_k = (-1)^k \Delta X \sum_{j=1}^{N} (-1)^j \phi_j \, e^{-i2\pi(k-1)(j-1)/N} \qquad (20)$$

For the inverse Fourier integral transform, the centered range of integration $\omega_1 = -M\Delta\omega$ to $\omega_{N+1} = M\Delta\omega$ is taken and, noting that $\bar{\phi}_{N+1} = \bar{\phi}_1^*$, the trapezoidal rule results in the finite sum

$$\phi_j = \frac{\Delta\omega}{2\pi}\left[\tfrac{1}{2}(\bar{\phi}_1 + \bar{\phi}_1^*) + \sum_{k=2}^{N} \bar{\phi}_k \, e^{i\omega_k X_j}\right]$$

$$= \frac{\Delta\omega}{2\pi}\left[\tfrac{1}{2}(\bar{\phi}_1^* - \bar{\phi}_1) + \sum_{k=1}^{N} \bar{\phi}_k \, e^{i\omega_k X_j}\right]$$

Since ϕ_1 is real and $(\bar{\phi}_1^* - \bar{\phi}_1)$ is imaginary, the result is

$$\phi_j = \mathcal{R}e\left[\frac{\Delta\omega}{2\pi} \sum_{k=1}^{N} \bar{\phi}_k \, e^{i\omega_k X_j}\right]$$

Substituting for ω_k and X_j from Eqs. (17) and (18), and again recalling that M is even, the inverse finite Fourier transform results:

$$\phi_j = \mathcal{R}e\left[(-1)^j \frac{\Delta\omega}{2\pi} \sum_{k=1}^{N} (-1)^k \bar{\phi}_k \, e^{i2\pi(k-1)(j-1)/N}\right] \qquad (21)$$

Eqs. (20) and (21) are best evaluated using the Cooley-Tukey FFT algorithm[18], for the reasons discussed above. In that case, M must be a power of 2.

The range of integration was approximately centered about the origin in both physical and spectral variables because of the symmetry property $\bar{\phi}(-\omega) = \bar{\phi}^*(\omega)$. The real variable $\phi(X)$ may be quite unsymmetrical, however, and aliasing errors may be observed. This effect arises because the non-periodic function $\phi(X)$ is represented by the finite Fourier transform as the periodic function $\phi(X)$, with period $N\Delta X$. Consequently, if an improperly aligned interval of length $N\Delta X$ is sampled from $\phi(X)$, aliasing may occur on either the left or right side of the sample interval. If on the left, for example, the aliased values actually would correspond to the correct values taken from $\phi(X)$ on the right of the interval. No such errors exist in $\bar{\phi}(\omega)$ as computed here, since the inertia terms are evaluated at each X-grid point independently. Aliasing does occur in the physical results, but is easily recognized since the flow properties decay to the undisturbed Blasius values at infinity. The effect can be avoided either by restricting the X-range of the data presented, or by use of a special inversion formula based on a properly uncentered integration interval. Both methods were used for the results presented in the following section. A better method of suppressing aliasing errors would be to evaluate the truncated tails of the Fourier integral by asymptotic analysis and add their contributions to the FFT result. This procedure is cumbersome and was not necessary for the cases dealt with here.

IV. Results

Two surface-height configurations, indicated by $H_1(X)$ and $H_2(X)$, have been

chosen to illustrate the spectral triple-deck method. The shapes are shown in Figure 1, and are defined by the relations

$$H_1(X) = \alpha/(1 + X^2)$$

$$H_2(X) = \begin{cases} 0 & \text{for } |X| > 1 \\ \alpha(1 - X^2)^2 & \text{for } |X| < 1 \end{cases}$$

The first of these shapes exhibits a long gentle variation of height, but has a Fourier transform that is much sharper, being significant only over a narrow range of ω:

$$\bar{H}_1(\omega) = \alpha\pi e^{-|\omega|}$$

The second shape has the opposite behavior: it differs from zero only over a narrow range, but has a slowly varying Fourier transform:

$$\bar{H}_2(\omega) = -16[3\omega\cos\omega + (\omega^2 - 3)\sin\omega]/\omega^5$$

with

$$\bar{H}_2(0) = 16/15$$

The opposing behavior of these two shapes in physical and spectral coordinates make them useful for case studies of the spectral method. The second shape $H_2(X)$ was used earlier by Sykes[21], and his finite-difference results will serve as a check case for incompressible flow. For supersonic flow, an independent check case was run for $H_1(X)$ using the time-marching finite-difference program of Jenson[9] and Rizzetta[10], modified to incorporate second-order accurate Crank-Nicolson differencing in X.

Figure 2 displays results for supersonic flow over the surface contour $H_1(X)$ for values of amplitude α from -3 to +3. (Positive α corresponds to a hump, negative α to a hollow in the surface.) The curves represent surface stress computed by the spectral program for $N_\omega = 128$, $\Delta X = 0.25$, $N_Y = 25$, $\Delta Y = 0.5$. The grid interval is obvious in the figure since values at grid points are connected by straight lines. The symbols are for the check-case results from the finite-difference program for $\alpha = -2$, with $N_X = 81$, $\Delta X = 0.25$, $N_Y = 37$, $\Delta Y = 0.25$. Obviously, the results of the two methods are in excellent agreement. The spectral method was much faster, however, requiring only 10 iterations for $\alpha = -2$, while the time-marching finite-difference program required 300 time steps to converge to the steady state. In terms of processing time, the spectral method is an order of magnitude faster, requiring for these cases about 10 seconds CPU time on an Amdahl 470/V6 computer verses about 81 seconds for the finite-difference program.

For the humps ($\alpha = 1,2,3$), the flow coming from the left at first decelerates, reducing the shear below the Blasius value ($\tau_o = 1$ in lower-deck scaling). For sufficiently tall humps ($\alpha > 7$, approx.) the flow would be expected to separate here, as well as on the lee side of the hump. Near the top of the hump the lower-deck flow is squeezed by the rapidly increasing surface height and the surface stress peaks to very high values. For the hollows ($\alpha = -1,-2,-3$) the reverse of these effects occurs. In this case, a flow-separation bubble occurs at the bottom of the hollow for $\alpha < -2.6$ (approx.). The non-linear effects can be seen in Figure 2, but are more clear in the table of values below, where the difference between the center-point shear and the Blasius value of unity is normalized with respect to α. The effect of non-linearity is demonstrated by the deviation from the value 0.537 for $\alpha = 0$. Clearly non-linearity is more important for the hollows than for the humps, accounting for a change of about 30% from the linear-theory value for $\alpha = -3$.

The effect of spatial resolution on accuracy is indicated in Figure 3 for $\alpha = -2$. The symbols represent results for a coarse grid having $N_\omega = 32$, $\Delta X = 1.0$, and the curve represents fine-grid results with $N_\omega = 128$, $\Delta X = 0.25$. (The fine-grid results are the same as those of Figure 2.)

For both grids $N_Y = 25$ and $\Delta Y = 0.5$. Both cases used the same X-range ($-16 \leq X \leq 16$, approx.), which is clearly large enough to yield accurate results. As N_ω is reduced below 32, with the same X-range, the accuracy degrades quickly owing to poor approximation to the surface shape for $\Delta X > 1$. Also reducing the X-range below about $-6 \leq X \leq 3$ severely degrades the accuracy, most likely due to truncation of the wake-like flow decay downstream.

TABLE I

SURFACE STRESS AT $X = 0$

$H(X) = \alpha/(1 + X^2)$

α	$\tau_0(0)$	$[\tau_0(0) - 1]/\alpha$
3	2.807	0.602
2	2.179	0.589
1	1.568	0.568
0	0.0	0.537
-1	0.508	0.492
-2	0.132	0.434
-3	-0.100	0.369

A comparison of separated supersonic-flow results with those for incompressible flow past the surface contour $H_1(X)$ is given in Figure 4. The amplitude $\alpha = -5$ was chosen for the comparison, since the incompressible flow does not separate for $\alpha < -4$. The incompressible flow (upper curve) converged in 30 iterations, but the supersonic flow (lower curve) did not converge to the same accuracy until 80 iterations. In the supersonic case, the residuals did not decay monotonically, and an under-relaxation factor of 0.5 was applied to obtain convergence. This case was the only one of those analyzed in this study that required under-relaxation. In general, the supersonic and incompressible flows show quite similar surface shear-stress patterns, especially in the separated region. It may be noted that the separated $\tau_0(X)$ distribution is very much like that computed for other configurations such as in the ramp study of Rizzetta, et al[10].

Our last comparison is for the quartic hump $H_2(X)$, which provides a severe test case for triple-deck computations. Sykes[21] considered incompressible flow past this shape as an example of topographic effects on the Earth's boundary layer; his results are compared here with results obtained spectrally. Ragab and Nayfeh[22] also obtained solutions for this shape with moderate amplitude ($\alpha \leq 2.4$), but reported that their finite-difference program would not converge for $\alpha = 3$, even with under-relaxation factors as small as 0.1. A similar failure was reported for Napolitano's[23] finite-difference scheme. The spectral method described here treated the problem with no difficulty, converging in 30 iterations without needing under-relaxation. The spectral results are shown in Figure 5 by the solid curve, and Sykes results are indicated by the symbols. The grid parameters are $N_\omega = 256$, $\Delta X = 0.125$, $N_Y = 31$, $\Delta Y = 0.5$ for the spectral results, and $N_X = 256$, $\Delta X = 0.08$, $N_Y = 60$, $\Delta Y = 0.25$, for the finite-difference results of Sykes. The two numerical solutions compare fairly well, with the spectral results displaying a smoother variation in the reversed flow region. There appears to be a slight oscillation in the finite-difference results, suggesting the need for a finer grid, already finer than that used in the spectral computations. It is interesting that both results show a sharp break in the slope of the shear-stress curve just downstream of the leading edge of the hump. These results for surface stress in incompressible flow appear qualitatively quite similar to those for supersonic flow past the $H_1(X)$ hump. The main difference is that the supersonic flow showed a stronger tendency to separate upstream of the hump, while the incompressible flow generates a rather large separation bubble in the lee of the $\alpha = -3$ hump. These trends would not appear to contradict physical insight

regarding the behavior of supersonic and incompressible flows.

V. Concluding Remarks

This study has demonstrated that the spectral method is fast and effective for solving triple-deck problems, with the ability to handle easily problems that some recent finite-difference methods are unable to solve. Moreover, the accuracy of the spectral method is compatible with that of the better finite-difference schemes. In this regard, it is often stated that the spectral method is of infinite-order accuracy, converging faster than any power of N. This statement would be true for finite domains if the boundary conditions did not introduce boundary discontinuities into the function represented by the Fourier series. Chebyshev polynomial representation is preferred for this reason.[19] For infinite domains, as in the present application, the Fourier integrals themselves lead to algebraic-order accuracy when discretized (2^{nd} order when using the trapezoidal rule). In addition, truncating the infinite range of integration leads to additional error depending on the asymptotic behavior of the physical and spectral functions involved. The use of too restricted a range of integration can lead to quite large errors. As can be seen from Eq. (19), the finite-range ($N\Delta X$) error in physical variables is equivalent to grid-size $\Delta\omega$ error in spectral variables, and vice versa. Consequently, it is necessary to use care in choosing grid size in both physical and spectral variables to ensure an accurate solution. Of course, similar considerations hold for finite-difference solutions.

References

1. Jobe, C. E., and Burggraf, O. R., Proc. Roy. Soc. London A340, 91-111, 1974.
2. Reyhner, T. A., and Flügge-Lötz, I., Int. J. Nonlinear Mech. 3, 173-199, 1968.
3. Smith, F. T., and Stewartson, K., J. Fluid Mech., 58, 143-159, 1973.
4. Davis, R. T., and Werle, M. J., Proc. 1976 Heat Trans. Fluid Mech. Inst., Stanford Univ. Press, 1976.
5. Williams, P. G., Proc. 4^{th} Int. Conf. Numerical Meth. in Fluid Dyn., Lecture Notes in Physics, Vol. 35, Springer-Verlag, Berlin, Heidelberg, and New York, 1975.
6. Lighthill, M. J., Proc. Roy. Soc. London A217, 478, 1953.
7. Stewartson, K., and Williams, P. G., Proc. Roy. Soc. London A312, 181-206, 1969.
8. Smith, F., and Stewartson, K., Proc. Roy. Soc. London A332, 1, 1973.
9. Jenson, R., Burggraf, O. R., and Rizzetta, D. P., Proc. 4^{th} Int. Conf. Numerical Meth. in Fluid Dyn., Lecture Notes in Physics, Vol. 35, Springer-Verlag, Berlin, Heidelberg, and New York, 1975.
10. Rizzetta, D. P., Burggraf, O. R., and Jenson, R., J. Fluid Mech. 89, 535-552, 1978.
11. Werle, M. J., and Vatsa, V. N., AIAA J. 12, 1491-1497, 1974.
12. Burggraf, O. R., Rizzetta, D. P., Werle, M. J., and Vatsa, V. N., AIAA J. 17, 336-343, 1979.
13. Messiter, A. F., SIAM J. Appl. Math. 18, 241, 1970.
14. Neiland, V. Ya, Akad. Nauk SSSR, Izv. Mekh. Zhidk. Gaza 3, 19, 1970.
15. Brown, S. N., Stewartson, K., and Williams, P. G., Phys. Fluids 18, 633-639, 1975.
16. Stewartson, K., Mathematika 16, 106, 1969.
17. Stewartson, K., Quart. J. Mech. Appl. Math. 23, 137-152, 1970, See also QJMAM 23, 1971.
18. Cooley, J. W., and Tukey, J. W., Math. Comp. 19, 297-301, 1965.

19. Orszag, S., Proc. 5th Int. Conf. Num. Methods Fluid Dyn., Lecture Notes in Physics, Vol. 59, Springer-Verlag, Berlin, Heidelberg, and New York, 1976.

20. Roache, P. J., J. Comp. Phys. 27, 204-220, 1978.

21. Sykes, R. I., Proc. Roy. Soc. London A361, 225-243, 1978.

22. Ragab, S. A., and Nayfeh, A. H., Paper No. 80-0072, AIAA 18th Aerospace Sciences Mtg, Jan 14-16, 1980.

23. Napolitano, M., Werle, M. J., and Davis, R. T., U. of Cincinnati, Dept of Aerospace Engrg. AFL Rpt. 78-6-42, 1978.

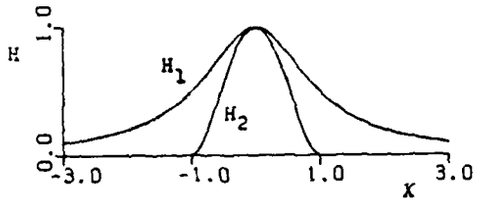

Figure 1. Surface Height Contours.

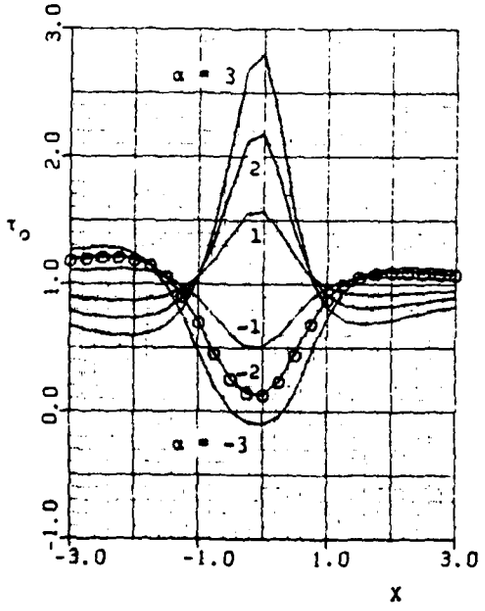

Figure 2. Surface Stress for Supersonic Flow Past Contour $H_1(X)$.

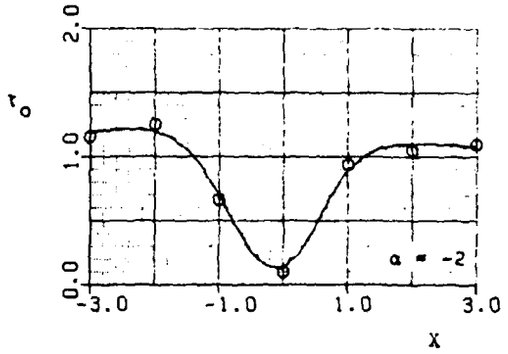

Figure 3. Effect of Grid Size on Accuracy; Supersonic Flow Past Contour $H_1(X)$.

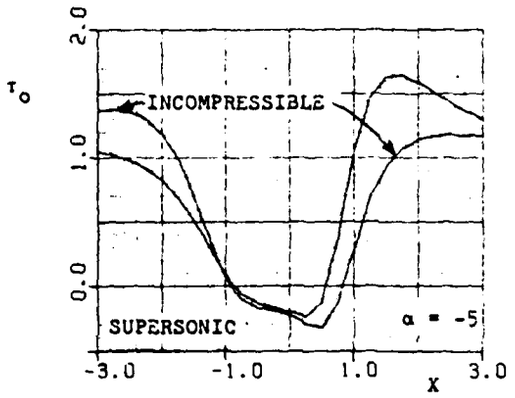

Figure 4. Comparison of Supersonic and Incompressible Flows Past Contour $H_1(X)$.

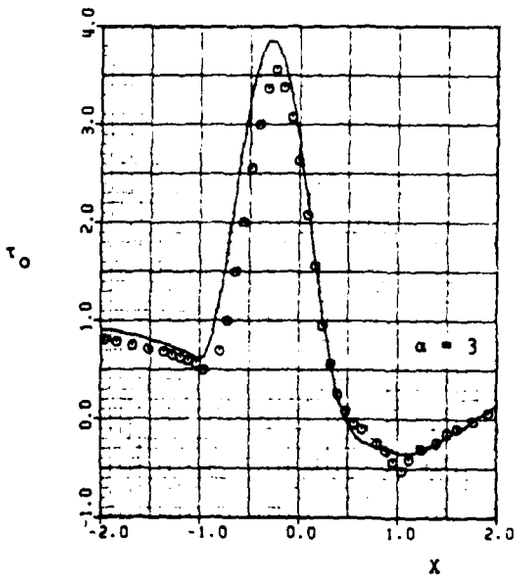

Figure 5. Surface Stress for Incompressible Flow Past Contour $H_2(X)$.

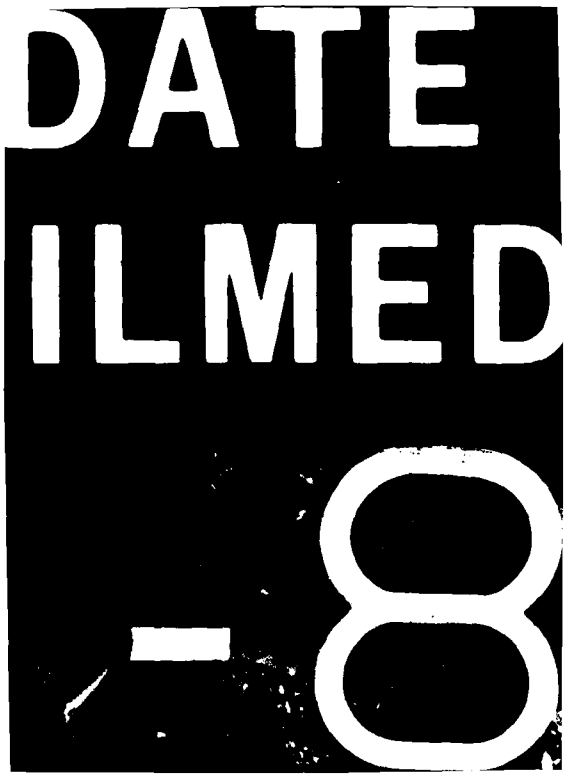
DATE
ILMED
-8